Effective Lemon Peels charcoal as a high adsorbent substance to purification and remove Fe (III) from water sources

[a]Fatima A. Al-Qadri*, [b]Jawaher Abdulrahman , [c]Abeer Yahia, [d]Naglaa Faleh

[a,b,c,d] Department of Chemistry, College of Science and Art in Sharurah, Najran University, Kingdome of Saudi Arabia

*Corresponding author`s e-mail: fatimaalqadri@gmail.com

Abstract

This study describes the creation of a low-cost activated carbon from lemon peels material extract as a precursor which is made from inexpensive lemon peels through a simple calcination process at 500°C and a green extraction with water. Nitrogen adsorption-desorption, FTIR analyses, and transmission electron microscopy were used to characterize the samples. The surface area of the obtained mesoporous lemon peels-derived activated carbon material was 282 m^2/g^1, and the pore size was 5.7 nm. For the adsorption of Fe (III) ions, an excellent adsorbent was obtained. Maximum Fe (III) ion adsorption capacity was 117.9 mg/g, and the effect of temperature, and time on its adsorption capacity were also investigated. The kinetic data fit the pseudo-second-order mode well, and the adsorption isotherms were confirmed with the Langmuir model. The thermodynamic results Negative values of G° indicate that the adsorption process was spontaneous, and negative values of entropy S° indicate that the state of the adsorbate at the solid/solution interface became less random during the adsorption process. According to the findings, prepared lemon peels-derived activated carbon has a high potential for removing heavy contaminating metal ions Fe(III) from aqueous solutions as a low-cost alternative to commercial adsorbents

Key words: Lemon peel, Fe (III), Adsorption, kinetic, Thermodynamic

1. Introduction

The release of large amounts of pollutants into the environment due to the rapid increase in industrial and agricultural activities is one of the key challenges globally [1]. Currently, one of the most important problems facing humans is environmental pollution. It was increased dramatically in the last few years and reached dangerous levels that threaten living organisms. The term heavy metal points to any chemical element with a comparatively high density and be toxic or poisonous at low concentrations [2]. Heavy metals are crucial pollutants in the water sources and industrial water-treatment. Hence, a severe public health issue is developing every day

by accumulating the heavy metals 'existence. Electroplating, finishing of metal, and metallurgical are some examples of the leading causes of these heavy metals and the chemical manufacturing, mining, and processes of battery manufacturing in large quantities. Heavy metals are recognized as toxic components, and their deposals through streams are causing unfavorable effects on the health of humans alike the environment [3][4][5]. High quality water is absolutely necessary to life of human; also, water with reasonable quality is important for domestic; agricultural; commercial, and industrial uses. From all above, it was observed that all these activities are responsible for water pollution. Every day huge quantities of waste are dumped from these sources into fresh water. The need of water is increasing as all resources of water slowly become unusable because of inappropriate disposal of waste [6]. The mission of providing suitable treatment facility for all sources of contaminated is hard and costly, so there is an urgent need for innovative, low-cost technologies that require low maintenance and energy efficient. Mostly, the use of different techniques is effective to remove heavy metals from water and wastewater [7, 9]; from these, sorption is efficient and economical [6]. Considered sorption onto activated carbon is a preferable method has been widely utilized in the past few years. Because of the urgent requirement to this treatment to be economic, the researchers intensified their efforts to finding and developing inexpensive alternatives available from various industrial, natural and biological materials or residues. Amidst these techniques, adsorption has great decontamination potential due to its tunability, versatility, and a wide variety of available sorbents [10, 11]. The efficiency of the adsorption technique is strongly reliant on the characteristics of the analyte, type of the adsorbent, and wastewater matrix composition. Lately, numerous scientists have explored the use of activated carbon derived from natural and low-cost agricultural wastes such as banana peels, orange peels, lemon peels, peanut shells, bamboo shoots, and coconut shells for the removal of dye contaminants from water [12]. One of the possible low-cost adsorbents is lemon peel. In addition, fruit peels or skins generally consist of lignin, cellulose, hemi-cellulose, carboxyl, hydroxyl, pectin substances, and amide surface functional groups which enhances the adsorbent-adsorbate interactions [13]. World citrus production was almost 140 million tons and growing, and orange production was reported to be 70 million tons in 2015 [14]. Both lemon and orange peel are no longer useful after the juice extraction and is free of charge from the processing industry, therefore, it is a preferred sorbent that has been studied by many researchers [15]. In this study as a result, carbon-rich agricultural residues will contribute to the negative environmental impacts when landfilled due to leachate that could lead to greenhouse gas emissions. Hence of, the manufacture of AC from waste materials, particularly agricultural residues would add economic value, reduce the cost and waste, and provide an economical alternative to commercial ACs. In order to remove Fe (III) from water sources, lemon peels and skins were used as precursors for

the manufacture of porous activated carbon. In comparison to the utilization of alternative commercially available carbon adsorbents, the conversion of biowaste to highly activated lemon peel carbon (LPAC) is both environmentally friendly and cost-effective. All adsorption studies were carried out, mass transfer on the material's surface is encouraged, and the interaction between the solute and the adsorbent is encouraged, all of which improve the adsorption effectiveness on the adsorption of different pollutants from aqueous solutions and have been documented. The result of different. The effect of various conditions, such as pH, adsorbent mass, and contact time, on the performance of the method was evaluated, and the optimal conditions were used to evaluate the isotherms and kinetics models

2. Materials and Method

Materials and Chemicals

Materials and reagents Ferric oxide, and sodium hydroxide (NaOH) were purchased from Merck, respectively. are analytical grades. 1000 mg /L of dye stock solution was made with redistilled water and diluted as needed to make a working solution.

Instrumentation and characterization

A Perkin-Elmer Lambda 35 spectrophotometer with 1.0 cm3 quartz cells and an 8 nm/sec scan speed was used to obtain spectrophotometric measurements. A Jenway 3305 pH meter and a glass-calomel electrode assembly calibrated with buffer solutions with pH values of 4.0 and 10.0—buffered by dissolving buffer capsules in second-generation de-ionized water—were used to measure the pH, which was accurate to 0.01 pH units. To mix the liquids, a Jenway 1000 magnetic stirrer was utilized. Additionally, the samples' surface functional groups were identified. The nitrogen (N_2) adsorption-desorption isotherms at 77.5 K were determined with a Quantachrome Instruments NOVA 2200e surface area and pore size analyzer. The BET (Brunauer-Emmett-Teller) method was used to determine the sample's specific surface area, and the pore size distribution was investigated.

Preparation of activation carbon adsorbent

A modified process was used to create activated carbon [16]. In a nutshell, lemons were bought at a nearby market, properly cleaned with deionized water, and dried separately for 24 hours at 100 °C. The dried skins were then broken down into particles with diameters between 100 and 300 mm. After the extra liquid was drained away, the material was dried for 12 hours at 100 °C in the oven. The carbon was then heated to 500 °C for three hours in a furnace. Distilled water was used to clean the

chemically activated carbon before it was dried at 100 °C. LPAC is the new name for the carbon that has been activated by lemon peel.

Adsorption Isotherm

Batch experiments were conducted with 0.5 g of activated carbon and 100 mL of Fe (III), solutions, with initial Fe (III), concentrations ranging from 100 to 400 mg/L. These were added to various conical flasks, and the adsorption took place for 24 hours at 60°C under normal pH conditions with continuous stirring. The equilibrium adsorption capacities of activated carbon for Fe (III), were calculated using the following equation:

$$q_e = \frac{(c_0 - c_e)\, x\, V}{w} \quad (1)$$

$$Removal\,(\%\,R) = \frac{C_o - C_i}{C_o} x\, 100 \quad (2)$$

where q_e is the equilibrium adsorption capacity (mg/g); C_0 and C_i are the initial and equilibrium concentrations (mg/L) of the Cu^{2+} solution, respectively; v is the volume of the initial solution (L) used for sorption; and W is the weight of the adsorbent (g).

Kinetic Adsorption

The kinetic reaction occurred and the equilibrium time was determined utilizing 0.5 g of sorbent at 70°C. The adsorption time varied from 30 to 120 min. The kinetics adsorption was estimated by two kinetic models: the pseudo-first-order model and pseudo-second-order mode

3. Results and discussion

FTIR spectroscopic studies

The samples' functional group changes were determined using FTIR. The extracted Activated Carbon. FTIR spectra were analyzed according to the steps shown in Fig. 1 [17]. The main characteristic peaks at 3000 and 3250 cm and 3300-3800 cm were assigned to (Si-O-Si), (Si-OH), and (Si-O-Si), respectively [18]. Fe (III) spectrum showed a main characteristic peak at 1560 and 2100 cm, and the formation of a metal oxygen bond caused the peak to appear at around 2100 cm.

The presence of metal coordination was confirmed by a strong band at 1000 cm, which corresponds to C-O-Fe stretching vibration [19].

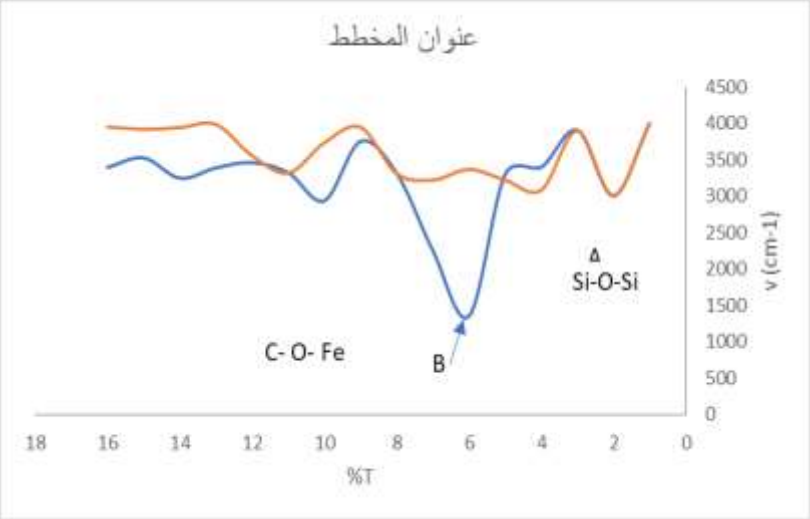

Fig. 1 FTIR of: (A) Lemon peel activated carbon (B) Fe (III)

Scanning Electron Microscope (SEM)

The surface morphology and elemental composition of the LPAC were investigated using SEM the images and spectrum are displayed in Figure 11. As seen from the SEM images in Figure 2 a, and b highly porous material, with surface pores, was successfully synthesized. This porous structure allows efficient adsorption as it offers adequate free spaces for target adsorbates.

Fig. 2. SEM images of (a), Lemon peel activated carbon (b) after adsorption of Fe (III).

Nitrogen Adsorption Desorption Analysis

As shown in Fig. 3, the functionalized activated carbon's N_2 adsorption isotherm produced a hysteresis loop in the p/p0 value range of 0.2 to 0.8, which is linked to capillary condensation, a property of mesoporous materials. The International Union of Pure and Applied Chemistry states that this proves activated carbon is a mesoporous substance with pores smaller than 50 nm in diameter [20]. The functionalized activated carbon was found to have a surface area of 236.36 m2/g, a pore size of 0.269 cm3/g, and a pore volume of 5.18 nm/nm using BET analysis.

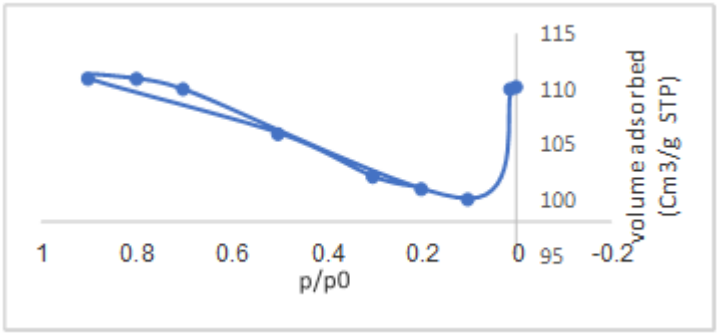

Fig.3. Adsorption/desorption isotherm of the functionalized Lemon peel activated carbon.

Adsorption Isotherms

Isotherms illustrate the equilibrium relationship between the concentration of adsorbate in the solution and the amount adsorbed on the adsorbent surface at a constant temperature. To fit experimental adsorption data, a variety of adsorption models are available in the literature. The adsorption isotherm displays the distribution of adsorption molecules between the liquid and solid phases once the adsorption process has reached an equilibrium condition. Finding a good model that can be applied to design is a crucial first step in fitting the isotherm data to various isotherm models. The equilibrium adsorption isotherm of Fe(III) ions onto lemon peel activated carbon is shown in Figure 4(a,b). It indicates that the adsorbed amount increases very little with increasing concentrations, showing a vertical increase at low concentrations and a horizontal plateau at higher values. As the initial Fe(III) concentration grew from 100 to 800 mg/L, the adsorption capacity at equilibrium (qe) increased from 38.98 mg/g to 159.168 mg/g, as illustrated in Fig. 4. At 800 mg/L of Fe (III) ion concentration, the maximum value of 117.9 mg/g was recorded. Fe (III) ion adsorption rose as the mass transfer driving force increased with starting concentration [21]. Similarly, [22] found that neem leaf powder has an adsorption effect on Cu (II) (NLP). Their results showed that, after reaching a maximum, the adsorption capacity rose with the initial Cu (II) ion concentration before declining as a

result of active group saturation. The results of the current investigation are in line with this.

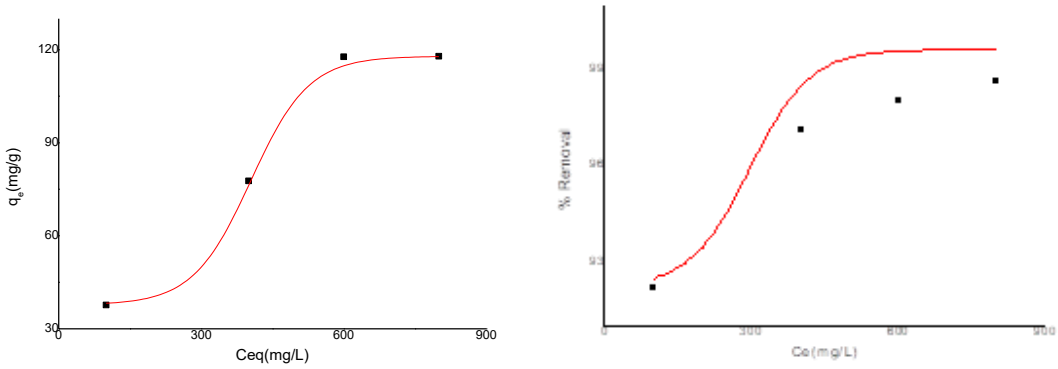

Figure 4. a) Adsorption isotherm of Fe (III) on the surface of lemon Peel Activated carbon, b) % Removal Fe (III)

Effect of adsorbent dosage on Fe (III) adsorption

As the adsorbent dosage was raised from 1 to 4 g, the Fe (III) removal percentage rose quickly, reaching 99% at the concentration of 600mg/L (Fig. 5). At a dosage of 4 g, the removal efficiency progressively reached adsorption equilibrium, and the amount of Fe (III) that was adsorbed did not increase further as the adsorbent was added. The adsorption potential of an adsorbent at a particular starting concentration is largely dependent on the adsorbent dosage. The accessible adsorption sites may be the main cause of the difference in adsorption capabilities at various adsorbent dosages. As the adsorbent dosage rose, more surface area and active sites became available for adsorption. Because it added unavailable sites, the higher adsorbent dosage had no effect on adsorbate absorption until adsorption achieved equilibrium [23, 24]. Moreover, the equilibrium concentration of Fe(III) was lower even though increasing the adsorbent dosage increased the interference of the adsorbent surface among the active groups. This occurred because there was insufficient driving force for the adsorbate to spread and bind to the adsorbent surface. These results are in line with other studies [25].

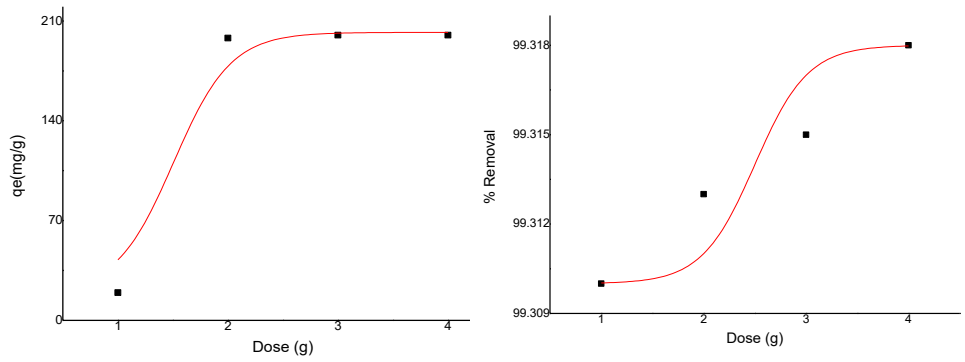

Fig 5. Effect of adsorbent dose of Fe (III) on the surface of lemon Peel Activated carbon b) %Removal of Fe (III)

Effect of time on adsorption of Fe(III)

Figure 6 illustrates the relationship between time and Fe(III) adsorption capacity as well as time and Fe(III)adsorption efficiency. The adsorption efficiency and capacity of Fe(III) increased with time, as Fig. 7 illustrates. There were two phases to the Fe(III)adsorption process using activated carbon: the initial reaction stage, which lasted from the start to the thirty-minute mark, and the subsequent stage. The primary mechanism of the first-stage reaction was surface adsorption, which accelerated the adsorption reaction and enhanced its capacity and efficiency. Gradual adsorption dominated the second reaction step. Relatively slowly, the adsorption reaction occurred. After 90 to 120 minutes, it steadily came to a state of balance. Fe (III) can be readily adsorbed by activated carbon because it is a mesoporous material with a strong mass transfer driving force in the early phases of adsorption and a large number of active sites. Nonlinear adsorption results from the accumulation of a significant amount of Fe(III) on the surface of activated carbon over time, which decreases the number of active sites and impedes Fe(III) mobility.

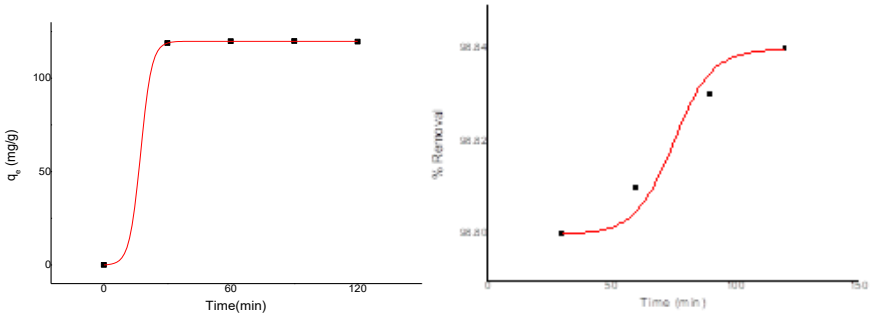

Fig 6. Effect of contact time on Fe (III) adsorption, on lemon Peel Activated carbon surface b)% Removal Fe(III)

Effect of Temperature

At an initial solution concentration of 40 mg/L, the adsorption of Fe (III) ions onto Activated carbon derived from lemon Peel was investigated at 343 K, 353 K, and 373 K. As illustrated in Fig. 7, the adsorption of Fe (III) metal ions onto Activated carbon increased from 118.81 mg/g at 343 K to 373 K. 119 mg/g at 373 K to 353 K The adsorbent's degradation altered the sorbent's surface chemistry, increasing the availability of functional groups that are active and reducing the adsorption of heavy metal ions. Moreover, the bonds switched in favor of the desorption process as temperatures increased [26]. Because metal ions leaked into the solution phase from the surface, limiting the adsorption capacity, the thickness of the boundary layer reduced as temperature rose [27].Similar results were achieved by Aksu et al. (2005), who found that when temperature increased from 25 to 45°C, the equilibrium absorption capacity of Cu (II) ions using dried sugar beet pulp as a sorbent reduced from 24.6 to 12.3 mg/g.

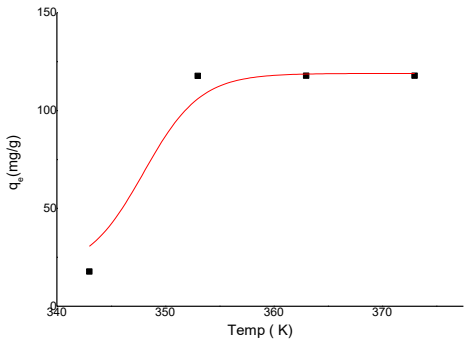

Fig 7. a) Effect of temperature of Fe (III) on the surface of lemon Peel Activated carbon

Adsorption Isotherms

Isotherms of Adsorption Two isotherm models—the Freundlich and Langmuir models—were used to determine the adsorption isotherms. As seen in Figs. 8 and 9, these two models were suitable for the Fe (III) adsorption process on the activated carbon in the lemon peel. Table 1 is a list of the data outcomes. The R^2 values were used as correlation coefficients by the isotherm equations that determined the adsorption process. In this study, the Freundlich and Langmuir isotherm models were applied.

Langmuir Isotherm

The Langmuir Isotherm While the Freundlich isotherm is an experimental equation used to represent heterogeneous systems, the Langmuir isotherm is based on the assumption of homogeneous adsorption. The findings showed that, for the adsorption examined in this work, the Langmuir model performed better than the Freundlich model. This implied that there was homogeneity in the adsorption process.

The maximum Fe (III) adsorption capacity was 142.9 mg/g, which was higher than or comparable to previously published data (Table 1). When C_e /q_e was plotted against C_e, a straight line with a slope of 1/q_e was obtained, as shown in Fig. 8. The results for the adsorption of Fe (III) ions onto lemon Peel Activated carbon were well fitted using the Langmuir isotherm, as demonstrated by an R^2 correlation value of 0.90. The Langmuir constants, b and q_{max}, which were connected to the adsorption energy and maximum adsorption capacity, respectively, were computed using the slope and intercept. The following formula represents the Langmuir isotherm, which denotes monolayer adsorption [28].

$$\frac{C_e}{q_e} = \frac{1}{q_{max} \cdot b} + \frac{1}{q_{max}} \cdot Ce \quad (3)$$

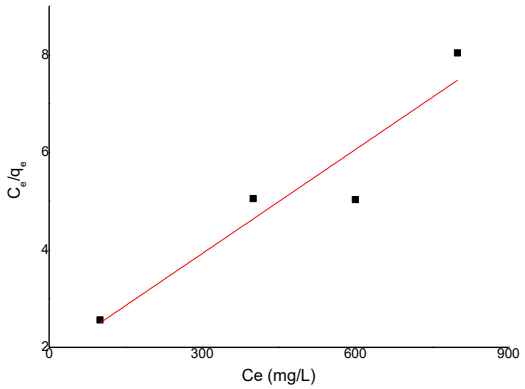

Fig. 8. Langmuir isotherm adsorption of Fe(III) on the surface of lemon Peel Activated carbon

The Langmuir isotherm's essential properties can be expressed in terms of a dimensionless equilibrium parameter (R_L) [29] The following is the definition of this parameter: Where C_i is the initial concentration of Fe(III) The R_L value indicates that the adsorption is unfavorable: R_L > 1; linear: R_L = 1; favorable: 0 < RL < 1; or irreversible: R_L = 0. Table 1 lists the Langmuir and Freundlich isotherm model parameters and correlation coefficients for the adsorption of Fe (III) ions on lemon Peel Activated carbon. R_L was found to be 0.0037, 0.00018, 0.00012, and 0.0092. These results emphasized that the Langmuir isotherm was the best at describing the adsorption of Fe (III) ions lemon Peel Activated carbon. The values of R_L were in the range of 0–1, which indicated that the adsorption of Fe (III) ions lemon Peel Activated carbon was favorable [30].

Freundlich Isotherm

The Freundlich isotherm is an experimental model where K_f and n are Freundlich constants that represent adsorption capacity and adsorption intensity, respectively, and q_e represents the amount adsorbed per amount of adsorbent at equilibrium (mg/g), C_e represents the equilibrium concentration (mg/L), and so on. The adsorbate has an impact on them as well.

Plotting ln q_e vs log Ce yields a straight line with slope n, which is the Freundlich equilibrium constants K_f and n. They also depend on the adsorbate if n is in the range of 1 to 10 (1/n is smaller than 1). Plotting ln q_e versus log C_e shows a straight line with slope n, which is the Freundlich equilibrium constants K_f and n. A number between 1 and 10 is thought to be advantageous for adsorption; the most common value is n > 1, which accounts for the distribution of active centers on the surface and any other feature that causes the adsorbent-adsorbate interaction to decrease as surface density increases. In the event that n falls between 1 and 10 (1/n is less than 1), metal ions have physically adhered to the lemon Peel Activated carbon. In the current investigation, n ranged from 1 to 10, indicating that metal ions were physically adsorbed onto the lemon Peel Activated carbon. It was valued at 4.67, and K_f was valued at 1.91. as displayed in Table 1 and Fig. 9. Equation (4) was used to compute the Freundlich constants K_f and n, which are given in Table 1. The favorability of adsorption is measured by the magnitude of n. The following equation represents the Freundlich model's logarithmic form [31]:

$$\log q_e = \log K_f + \frac{1}{n} \log C_e \qquad (5)$$

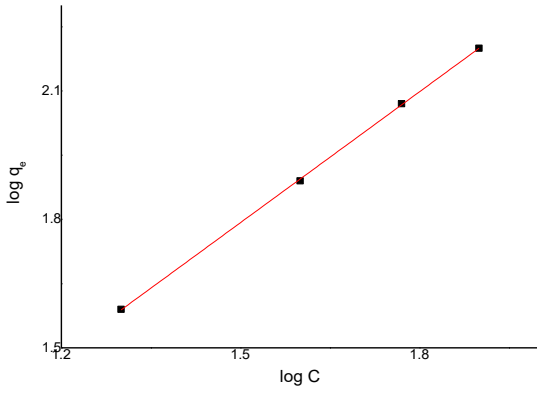

Fig. 9. Freundlich isotherm adsorption of Fe (III) on the surface of lemon Peel Activated carbon

Table 1. Parameters of Langmuir and Freundlich isotherms for adsorption of Fe(III) ions onto (LPAC) Lemon peels activated carbon surface

Langmuir			Freundlich		
q_{max} (mg/g)	b (L/mg)	R^2	n	K_f	R^2
142.9	1.11	0.90	1	0.26	0.78

Adsorption kinetics studies

Kinetics of Adsorption The properties and mechanism of adsorption, as well as the rate-limiting step throughout the adsorption process, have been understood through the application of several adsorption kinetic models, including the pseudo-first-order and pseudo-second-order models.[32]

The pseudo-first-order model was suggested by [33] The linear form of the pseudo-first-order model is expressed as follows:

$$ln(q_e - q_t) = lnq_e - k_1 .t \quad (6)$$

where q_e and qt (mg/g) are the amounts of Fe (III) ions adsorbed onto lemon Peel Activated carbon at equilibrium and time t, respectively; and K_1 (min^{-1}) is the rate constant of the pseudo-first-order kinetic model. A straight line was obtained by plotting ln (q_e - q_t) against time. This straight line was used to determine -K_1, correlation coefficient R^2, and the theoretical value of q_e. Although the plot was linear and the calculated value (q_e, calc.) and experimental value (q_e, exp.) were not in agreement with each other, the values of the correlation coefficient for the pseudo-first-order kinetic model were smaller than those of the pseudo-second-order kinetic model. Thus, the adsorption kinetics for the pseudo-first-order kinetic model were poor, as shown in Fig. 10 and Table 2.

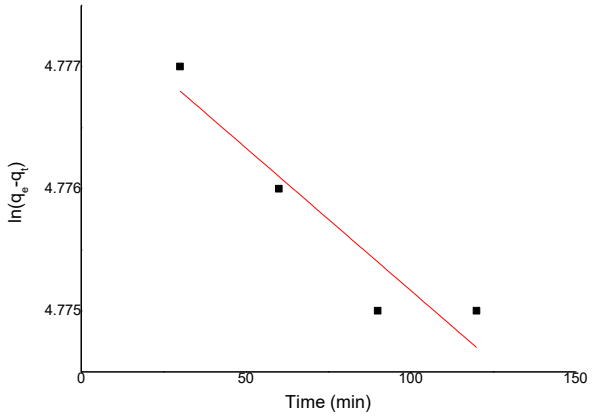

Fig. 10. Pseudo-first-order of Fe (III) on the surface of lemon Peel Activated carbon

Pseudo-second-order reaction

$$\frac{t}{q_t} = \frac{1}{k_2 q2_e} + \frac{1}{q_e} .t \qquad (7)$$

Figure 11 shows the typical graphs for the pseudo-second order equation. The outcomes show that the pseudo-second-order binding mechanism predominates and that the chemisorption step is used to adsorb the Fe (III) LPAC adsorbent. This involves the valence force through the exchange of electrons between the dyes and adsorbent. Furthermore, there is a strong affinity between the adsorbent and the Fe (III). The quick half-adsorption time obtained with the majority of the Fe (III) removed illustrates this.

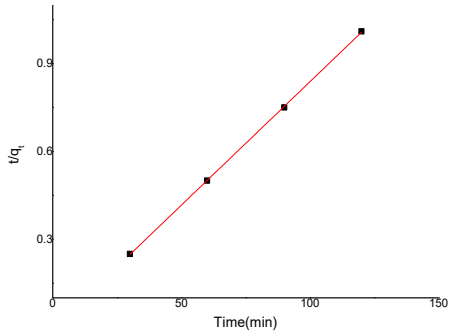

Fig. 11. Pseudo-second-order of Fe (III) on the surface of lemon Peel Activated carbon

Table 2. Kinetic parameters and correlation coefficients of two kinetic equations for different initial Fe (III) ion concentrations on lemon Peel Activated carbon

Metal ion	$q_{e,exp}$ mg/g	First-order kinetic mode			Second-order kinetic mode		
Fe (III)	117	$q_{e,cal}$ (mg/g)	K_1 min	R^2	$q_{e,cal}$ (mg/g)	K_2 g/g.min	R^2
		4.777	$-2.33x10^{-5}$	0.88	119	0.996	0.99

Thermodynamic Parameters

The thermodynamic parameters that determined the process were changes in the standard enthalpy (H°), standard entropy (S°), and standard free energy (G°) due to the transfer of a unit mole of solute from the solution onto the solid–liquid interface. The values of H° and S° were calculated using the following equations:

$$lnkc = \frac{\Delta S}{R} - \frac{\Delta H}{RT} \qquad (8)$$

$$\Delta G = -RTlnK \qquad (9)$$

where R is the universal gas constant (8.314 J/(mol.K); T (K) is the absolute temperature in Kelvin, and Kc is the linear adsorption distribution coefficient, which is defined as follows: $K_c = C_o/C_e$, where C_o and C_e (mg/L) are the initial adsorbate concentration and concentration of the adsorbate remaining in the liquid phase at equilibrium, respectively. ΔG° is the free energy of adsorption, ΔH° (kJ/mol) is the enthalpy change, and ΔS° (J/(mol. K)) is the entropy change. The values of H° and S° were calculated from the slope and intercept of the plot for log K versus Temp in Kelvin and it is shown in Figure 12.Figure 12 depicts the values of H° and S° as determined from the slope and intercept of the log K versus Temp plot in keleven plot. The information on the thermodynamic parameters was gathered and is shown in Table 3. An associative mechanism participated in the adsorption process, as indicated by a negative result for ΔS°. In this instance, the adsorption occurred as a result of the adsorbent and adsorbate forming an activated complex [34]. The entropy ΔS° value indicated a decrease in the degrees of freedom for the Fe (III) ions in the solution as well as a change in the state of the adsorbate at the solid/solution interface during the adsorption process, with ΔS° < 0 or > 0. When the temperature increased, ΔG° showed a positive value, indicating that the adsorption process was not spontaneous. Conversely, a negative value indicated that the adsorption process was spontaneous.

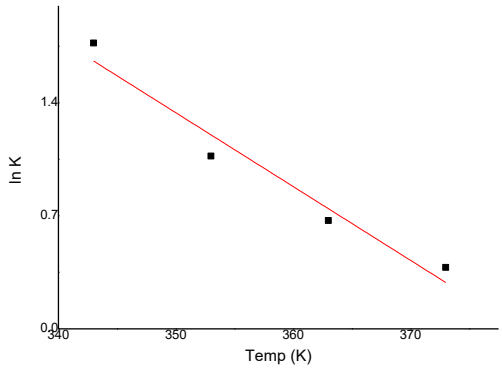

Figure 12 . Effect of temperature of Fe (III) on the surface of lemon Peel Activated carbon.

Table 3. Thermodynamic parameters for adsorption Fe (III) on the surface of lemon Peel Activated carbon			
T (K)	ΔG° (J/mol)	ΔH° (J/mol)	ΔS° (J/mol.k)
343	-33.88.	-73	-140.72
353	-85.48		
363	-60.36		
393	-46.83		

Conclusions

It was investigated how to remove it from synthetic water samples using an LPAC adsorbent. The two most important factors influencing the sorption of Fe (III) from water sources were the pH and the bulk of the adsorbent. The Langmuir isotherms and pseudo-second-order reaction rate model provided the best description of the isotherms and kinetics results on the sorption of Fe (III) from water sources. 117.9 mg/g of Fe (III) might be adsorbed from water sources, according to the results. Thus, the process involving LPAC adsorbent and Fe (III) was electrostatic attraction. While the chemisorption adsorption mechanism of dyes onto the LPAC adsorbents is suggested by pseudo-second order to utilize its adsorption capability, the LPAC material can be recovered up until the fifth cycle. These might be directed. These could be referred to as a good cleaning technology for Fe (III) adsorption. The maximum removal efficiencies of Fe (III) in water samples ranged from 96 % to 98.4 %. Furthermore, the outcomes received shows that LPAC could be a possible adsorbent for the adsorption process of Fe (III). In order to obtain basic engineering data on adsorbents for field operation, fixed-bed continuous operation is required. Further studies should focus on the application of activated carbon material derived from lemon peels on continuous adsorption study using batch technology. It is a good technology that has been previously applied in the removal of various pollutants such heavy., the outcomes received shows that LPAC could be a possible adsorbent for the adsorption process of Fe (III). In order to obtain basic data on adsorbents for field operation

Conflict of Interest

All authors approve the final manuscript and declare that there is no conflict of interest.

Acknowledgment

The authors are thankful to the Deanship of Scientific Research at Najran University for funding this work under the Future Funding program grant code (NU/SRP/SERC/12/6)

REFERENCES

1. Ahmadi, Sajad, and Hossein Ganjidoust. "Using banana peel waste to synthesize BPAC/ZnO nanocomposite for photocatalytic degradation of Acid Blue 25: Influential parameters, mineralization, biodegradability studies." *Journal of Environmental Chemical Engineering* 9.51,06010 (2021)
2. Paksamut, J., and P. Boonsong. "Removal of copper (II) ions in aqueous solutions using tannin-rich plants as natural bio-adsorbents." *IOP Conference Series: Materials Science and Engineering*. Vol. 317. No. 1. IOP Publishing, (2018).
3. P. Senthil Kumar, K. Krithka. ―Kinetics and Equilibrium Studies of Zn^{2+} Ions Removal from Aqueous Solutions by Use of Natural Waste‖, Electronic Journal of Environment, Vol. 9, no. 1, pp. 264- 274 (2010).
4. Lahieb Faisal M. ―Batch Sorption of Copper (II) Ions from Simulated Aqueous Solution by Banana Peel‖, Al-Khwarizmi Engineering Journal, Vol. 12, no. 4, pp. 117-125 (2016).
5. Maryam Q Al-Qaisi, Lahieb Faisal M.A., Zainab T. Al-Sharify., Talib A. Al-Sharify. ―Possibility of Utilizing from Lemon Peel as a Sorbent in Removing of Contaminant Such as Copper Ions from Simulated Aqueous Solution‖, International Journal of Civil Engineering and Technology (IJCIET) , Vol. 9, no. 11, pp. 571-579 (2018) .
6. JALALI, Mohsen; ABOULGHAZI, Fathemeh. Sunflower stalk, an agricultural waste, as an adsorbent for the removal of lead and cadmium from aqueous solutions. *Journal of Material Cycles and Waste Management*, 15: 548-555. (2013)
7. ESALAH, Jamaleddin O.; WEBER, Martin E.; VERA, Juan H. Removal of lead, cadmium and zinc from aqueous solutions by precipitation with sodium Di-(n-octyl) phosphinate. *The Canadian Journal of Chemical Engineering*, , 78.5: 948-954 (2000).
8. CANET, L.; ILPIDE, M.; SETA, P. Efficient facilitated transport of lead, cadmium, zinc, and silver across a flat-sheet-supported liquid membrane mediated by lasalocid A. *Separation Science and Technology*, , 37.8: 1851-1860,(2002).
9. DIMPE, K. Mogolodi; NOMNGONGO, Philiswa N. A review on the efficacy of the application of myriad carbonaceous materials for the removal of toxic trace elements in the environment. *Trends in Environmental Analytical Chemistry*, 16: 24-31(2017).
10. Mashile, Geaneth Pertunia, Anele Mpupa, and Philiswa Nosizo Nomngongo. "Magnetic mesoporous carbon/β-cyclodextrin–chitosan nanocomposite for extraction and preconcentration of multi-class emerging contaminant residues in environmental samples." Nanomaterials 11.2: 540. (2021).
11. Ahmadi, Sajad, and Hossein Ganjidoust. "Using banana peel waste to synthesize BPAC/ZnO nanocomposite for photocatalytic degradation of Acid Blue 25:

Influential parameters, mineralization, biodegradability studies." Journal of Environmental Chemical Engineering 9.5106010 : (2021)

12. Pandiarajan, Aarthi, et al. "OPAC (orange peel activated carbon) derived from waste orange peel for the adsorption of chlorophenoxyacetic acid herbicides from water: adsorption isotherm, kinetic modelling and thermodynamic studies." *Bioresource technology* 261, 329-341: (2018).
13. Gunay Gurer, Ayse, et al. "Adsorption isotherms, thermodynamics, and kinetic modeling of methylene blue onto novel carbonaceous adsorbent derived from bitter orange peels." *Water, Air, & Soil Pollution* 232 , 1-17 : (2021).
14. Bukhari, Aysha, et al. "Removal of Eosin dye from simulated media onto lemon peel-based low cost biosorbent." *Arabian Journal of Chemistry* 15.7 ,103873 : (2022).
15. Cheng, S., Zhao, S., Xing, B., Liu, Y., Zhang, C., Xia, H., 2022. Preparation of magnetic adsorbent-photocatalyst composites for dye removal by synergistic effect of adsorption and photocatalysis. J. Clean. Prod. 348, 131301: (2021),
16. GUGUSHE, Aphiwe Siyasanga, et al. Adsorptive removal of Cd, Cu, Ni and Mn from environmental samples using Fe3O4-zro2@ APS nanocomposite: kinetic and equilibrium isotherm studies. *Molecules*, 26.11: 3209: (2021)
17. Umeda, J. & Kondoh, K.High-purification of amorphous silica originated from rice husks by combination of polysaccharide hydrolysis and metallic impurities removal. Industrial Crops and Products, 32 (3): 539–544 (2010):
    DOI 10.1016/j.indcrop.2010.07.002
18. Fernandes, I.J., Calheiro, D.F., Sάnchez, A.L., Camacho, A.L.D., de Campos Rocha, T.L.A., Moraes, C.B.A.M. & de Sousa, V.C.Characterization of Silica Produced from Rice Husk Ash: Comparison of Purification and Processing Methods. Materials Research, Vol 20(2), pp. 512–518 (2016):
    DOI: 10.1590/1980-5373- MR-2016-1043.
19. Blitz, I.P.; Blitz, J.P.; Gun'ko, Z. M.; Sheeran, D.J Functionalized silicas: Structural characteristic and adsorption of Cu(II) and Pb(II). Colloids Surf. A: Physicochem. Eng. Aspects, 307, 83 (2007)
    DOI: 10.1016/j.colsurfa.2007.05.016
20. Ali, Nisreen S., et al. "Adsorption of methyl violet dye onto a prepared bio-adsorbent from date seeds: Isotherm, kinetics, and thermodynamic studies." *Heliyon* , ,8.8: e10276 (2022).
21. Syafiqa Ayob , Norzila Othman, Wahid Ali Hamood Altowayti , Faisal Sheikh Khalid1 ,Norshila Abu Bakar, Muhammad Tahir , Eddy Setiadi Soedjono, A Review on Adsorption of Heavy Metals from Wood-Industrial Wastewater by Oil Palm Waste.. Journal of Ecological Engineering, , 22(3), 249–265 (2021)
22. KKIU Arunakumara Buddhi Charana Walpola,Min-Ho Yoon,Banana Peel: A Green Solution for Metal Removal from Contaminated WatersI., Korean J Environ Agric. Vol. 32, No. 2, pp. 108-116 (2013).
23. Elsayed, A., Osman, D., Attia, S., Ahmed, H., Shoukry, E., Mostafa, Y. & Taman, A. A Study on the Removal Characteristics of Organic and Inorganic Pollutants from Wastewater by Low Cost Biosorbent. Egyptian Journal of Chemistry, 63(4), pp. 1429–1442 ,15710.1950 ((2020).
    DOI: 10.21608/ejchem.2019.15710.1950.

24. Mahmudi, M., Arsad, S., Amelia, M.C., Rohman-ingsih, H.A. & Prasetiya, F.S. An alternative activated carbon from agricultural waste on chromium removal. Journal of Ecological Engineering, 21(8), 1–9.((2020). DOI: 10.12911/22998993/127431
25. Park, D., Lim, S.R., Yun, Y.S. & Park, J.M. Development of a new Cr(VI)-biosorbent from agricultural biowaste. Bioresource Technol. l 99: 8810–8818. DOI: 10.1016/j. biortech.2008.04.04 (2008).
26. Sharaf, G. & Hassan, H. Removal of copper ions from aqueous solution using silica derived from rice straw: comparison with activated charcoal. International Journal of Environmental Science and Technology. (2014). DOI: 10.1007/s13762-013-0343-8
27. El-Araby, H. A., Ibrahim, A.M.M.A., Mangood, A.H., & Adel, A.H. Sesame husk as adsorbent for copper (II) ions removal from aqueous solution. Journal of Geoscience and Environment Protection, 5(07), 109 (2017). DOI: 10.4236/gep.2017.57011
28. Langmuir, I. The Constitution and Fundamental Properties of Solids and Liquids. Part I. Solids. Journal of the American Chemical Society, 38, 2221–2295 (1916). DOI: 10.1021/ja02268a002.
29. Owoeye, S. S., Toludare, T.S., Isinkaye, O.E. & Kingsley, U. Influence of waste glasses on the physico-mechanical behavior of porcelain ceramics. Boletín de la Sociedad Española de Cerámica y Vidrio, 58(2), 77–84 (2019). DOI: 10.1016/j.bsecv.2018.07.002
30. El-Araby, Haitham Ahmed, et al. "Sesame husk as adsorbent for copper (II) ions removal from aqueous solution." Journal of Geoscience and Environment Protection 5.07 : 109 (2017)
31. Freundlich, H. Über die adsorption in lösungen. Zeitschrift für physikalische Chemie, 57(1), 385-470 (1907).
32. Taha, A.A., Ahmed, A.M., Abdel Rahman, H.H., Abouzeid, F.M. & Abdel Maksoud, M.O. Removal of nickel ions by adsorption on nano-bentonite: Equilibrium, kinetics, and thermodynamics. J. Dispers. Sci. Technol., 38, 757–767 (2017). DOI: 10.1080/01932691.2016.1194211
33. Gupta, V.K., Gupta, M. & Sharma, S. Process development for the removal of lead and chromium from aqueous solutions using red mud—an aluminium industry waste. Water research, 35(5), 1125–113 , 35 (2001).
34. Aregawi, B.H. & Mengistie, A.A. Removal of Ni (II) from aqueous solution using leaf, bark and seed of moringa stenopetala adsorbents. Bulletin of the Chemical Society of Ethiopia, 27:35. (2013) :: DOI: 10.4314/bcse.v27i1.4